Acta Crystallographica Section A
Foundations of Crystallography
ISSN 0108-7673

Received 19 December 2006
Accepted 11 March 2007

© 2007 International Union of Crystallography
Printed in Singapore – all rights reserved

Size-dependent interbranch peculiarities of X-ray extinction in strongly bent crystals

Michael Shevchenko

Institute for Metal Physics, 36 Vernadsky Street, 03142 Kiev, Ukraine. Correspondence e-mail: mishevch@yahoo.com

X-ray diffraction from homogeneously bent crystals is studied within the interbranch resonance concept for large gradient. It is shown that strong deformations lead to an interbranch phase modulation of the transmitted and diffracted waves. It is predicted that prominent extinction effects occur due to the interbranch phase changes. These features are very sensitive to the crystal thickness, so that changes of the order of the interbranch extinction length can affect considerably the rocking-curve structure. Numerical calculations of the diffracted intensity are carried out to illustrate this.

1. Introduction

The X-ray dynamical diffraction in a crystal with a uniform strain gradient has been investigated in many theoretical and experimental works [they are reviewed in detail by Authier (2005)]. From the diffraction phenomena derived from these studies, of special interest is the X-ray interbranch scattering, predicted first by Penning (1966). It is worth pointing out that this effect is due to lattice distortions and it disappears for a perfect crystal. As the value of the strain gradient enlarges, the interbranch scattering increases resonantly. This process is accompanied by violation of Kato's Eikonal theory and significant intensification of 'new' wavefields whose tiepoints belong to another dispersion branch than those which are propagating (Authier & Balibar, 1970; Balibar *et al.*, 1983).

In the case of strong deformation, the X-ray diffraction occurs in a small thickness range, which is considerably less than the X-ray extinction length ξ_g for an ideal crystal. This implies the kinematical approach to X-ray scattering. In this connection, we pay attention to the fact that all extinction effects for real crystals, which consist of mosaic blocks statistically misoriented with respect to one another, are neglected in the kinematical approximation (Zachariasen, 1967). Only in the successive approximation which rejects solely the 'feedback' term of the equations for the transmitted power does the correction on the secondary extinction (Darwin, 1922) appear for small mosaic blocks. However, the atoms in a bent crystal are displaced in a regular and well defined fashion, such that even in a highly distorted crystal the scattered waves must be regarded as perfectly coherent with the incident wave. As a result, the waves diffracted by the different atoms will interfere constructively by involving the phase relations among themselves. Thus, the X-ray multiple scattering which influences the phases of the reflected waves ought to be manifested in the diffracted intensity from a strongly bent crystal.

It is necessary to observe that the link between the interbranch scattering and the extinction caused by a regular strain field in a single coherent domain has been established for ideal thickness variation (Kuriyama & Miyakawa, 1970). The changes of the diffracted intensity from the dynamical to the kinematical value as a function of the degree of crystal imperfections were studied in that case. It was also shown that the passage from dynamical to kinematical scattering is described by an extinction term which is due to the interbranch transitions. From this viewpoint, we consider as well the extinction problem for a strongly bent crystal. Applying the interbranch resonance concept (Shevchenko, 2005), we are going to find the correlation between extinction effects and interbranch scattering of X-rays in the crystal. Obviously, such 'fine-structure' effects will reflect the violation of the principle of local 'lattice homogeneity' inherent in a weakly deformed crystal.

2. Basic equations

Assuming a one-dimensional distortion, the equations of the dynamical diffraction theory have the following form (Hirsch *et al.*, 1977):

$$\begin{cases} \dfrac{\mathrm{d}D_0(z)}{\mathrm{d}z} = \dfrac{i\pi}{\xi_g} D_g(z) & (1) \\ \dfrac{\mathrm{d}D_g(z)}{\mathrm{d}z} = \dfrac{i\pi}{\xi_g} D_0(z) + i\left[s + \mathbf{g}\dfrac{\mathrm{d}\mathbf{u}}{\mathrm{d}z}\right] D_g(z), & (2) \end{cases}$$

where $D_{0,g}(z)$, s and $\mathbf{u}(z)$ stand for the amplitudes of the transmitted and diffracted waves, the deviation from the point in the reciprocal space and a displacement field which depends only on the depth z inside the crystal, respectively. It is convenient to expand the amplitudes D_0 and D_g over the Eikonal basic functions:

$$D_{0,g}(z) = \exp\left\{ i \int_0^z q(z_1)\,\mathrm{d}z_1 \right\} \sum_{j=1,2} A^j_{0,g}(z) \Phi^j_{0,g}(z), \qquad (3)$$

where $q(z) = [s + \mathbf{g}\,\mathrm{d}\mathbf{u}(z)/\mathrm{d}z]/2$, $A_{0,g}^{1,2}(z)$ and $\Phi_{0,g}^{1,2}(z)$ are the modulation amplitudes and the Eikonal solutions for the transmitted and diffracted waves of equations (1) and (2) for the 'upper' and 'lower' dispersion branches, respectively. Expression (3) introduces the Eikonal representation of the dynamical theory. This expansion simplifies the analysis of the X-ray interbranch scattering by extracting the into-a-branch contribution from the amplitudes of the wavefields. In the symmetrical Laue case, the fundamental equations for the modulation amplitudes corresponding to the wave $D_0(z)$, subjected to the interbranch crossover, are given by (Shevchenko, 2005)

$$\frac{\mathrm{d}A_0^{1,2}(z)}{\mathrm{d}z} = -\frac{A_0^{2,1}(z)\exp\left\{\mp(2i\pi/\xi_g)\int_0^z p(z_1)\mathrm{d}z_1\right\}}{2p^2(z)\{\omega \pm [1+\omega^2]^{1/2}\}}\frac{\mathrm{d}\eta(z)}{\mathrm{d}z}. \quad (4)$$

Here $p(z) = [1+\eta^2(z)]^{1/2}$, where the deviation $\eta(z) = \omega + (\mathbf{g}\,\mathrm{d}\mathbf{u}/\mathrm{d}z)\xi_g/(2\pi)$ and $\omega = s\xi_g/(2\pi)$. For the sake of simplicity, we consider a homogeneous bending $u(z) = \alpha z^2/(2R)$, where R ($R > 0$) and α are the radius of curvature and a constant describing the deformation, respectively. It is worth observing that the values ω and $\alpha\cos\beta$, where β is the angle between $\mathbf{g}$ and $\mathbf{u}$ vectors, must have opposite signs for the interbranch crossover occurrence. For practical purposes, we shall assume that $\alpha\cos\beta > 0$. Then, the deviation parameter $\eta(z) = \varepsilon\pi(z - z_0)/\xi_g$, where $\varepsilon = \alpha g\xi_g^2\cos\beta/(2\pi^2 R)$ and z_0 corresponds to the point where Bragg's condition is locally satisfied

In the vicinity $\tilde{z}$ of any point z_s, we approximate $u(z) \approx u(z_s) + u'(z_s)\tilde{z}$, where $z - z_s = \tilde{z}$. With this in mind, equation (4) can be reduced in this range to

$$\frac{\mathrm{d}^2A_0^{1,2}(\tilde{z})}{\mathrm{d}\tilde{z}^2} \pm \frac{2i\pi}{\xi_g}p_s\frac{\mathrm{d}A_{1,2}(\tilde{z})}{\mathrm{d}\tilde{z}} + \left(\frac{\varepsilon\pi}{2\xi_g}\right)^2\frac{A_0^{1,2}(\tilde{z})}{p_s^4} = 0, \quad (5)$$

where $p_s = [1+\eta_s^2]^{1/2}$ and $\eta_s = \eta(z_s)$. It should be noted that $\eta(z)$ is a linear function of $u'(z)$. Therefore, considering $u'(z)$ as constant within a small region near z_s, $\eta(z)$ and $p(z)$ are also considered to be constant η_s and p_s in that region. Using equation (5), one can obtain the following expressions for the modulation amplitudes $A_0^{1,2}$:

$$A_0^{1,2}(z) = C_{1,2}^{+}(z_s)\exp\{i(Q_s \mp W_s)z\} + C_{1,2}^{-}(z_s)\exp\{i(-Q_s \mp W_s)z\}. \quad (6)$$

Here $Q_s = [W_s^2 + (\pi/L_s)^2]^{1/2}$, $W_s = \pi p_s/\xi_g$, $L_s = 2\xi_g p_s^2/\varepsilon$. Expression (6) describes the drastic changes of the local dispersion surface in a highly deformed crystal. Owing to the interbranch interchange, the dispersion branches '1' and '2' split into the 'new' waves $1^{\pm}$ and $2^{\pm}$ with the wavevectors $P_{s,1}^{\pm} = -W_s \pm Q_s$ and $P_{s,2}^{\pm} = W_s \pm Q_s$, respectively, which have amplitudes $C_{1,2}^{\pm}(z_s)$. It should be noted that the interbranch dispersion anomalies can also be specified with the help of 'new' Bloch modes $\psi_B^{\pm}$. By analogy with the conventional dynamical theory, it is possible to introduce such waves by combining the 'new' 'upper' ('lower') branches 1^+ (1^-) and 2^+ (2^-), respectively.

In the case of the interbranch crossover caused by the strong deformations $\varepsilon \gg 1$, it was shown in Shevchenko & Pobydaylo (2005) that near z_0 the energy transfers from the wave ψ_B^+ to the wave ψ_B^-. In doing so, we will neglect any attenuation of the incident wave through the crystal by diffraction. Then, adding only the local phase multipliers $\pm Q_s z$ associated with the 'new' modes $\psi_B^{\pm}$, from (3) and (6), the expressions for the transmitted wavefield follows for $z < z_0$ and $z > z_0$, respectively:

$$D_0(z) = \begin{cases} \exp\left\{i\int_0^z [q(z_1) + Q(z_1)]\,\mathrm{d}z_1\right\}, & z < z_0 \\ \exp\left\{i\int_0^z [q(z_1) - Q(z_1)]\,\mathrm{d}z_1\right\}, & z > z_0. \end{cases} \quad (7)$$

From (7), it appears that the changing of the sign of the function $Q(z)$ takes place in the expression for $D_0(z)$ owing to the jump of the tiepoint. In the kinematical approximation, within which (7) is correct, extinction of X-rays was mentioned above to be absent for a mosaic crystal. However, multiple scattering effects can appear prominently in the beam diffracted by a strongly bent crystal. To show this, we will integrate equation (2) and write the following expression for the amplitude of the diffracted wave:

$$D_g(z) = \frac{i\pi}{\xi_g}\exp\left\{2i\int_0^z q(z_1)\,\mathrm{d}z_1\right\} \times \int_0^z \exp\left\{-2i\int_0^{z_2} q(z_1)\,\mathrm{d}z_1\right\} D_0(z_2)\,\mathrm{d}z_2. \quad (8)$$

Substituting (7) into (8), one gets

$$D_g(z) = \frac{i\pi}{\xi_g}\exp\left\{2i\int_0^z q(z_1)\,\mathrm{d}z_1\right\} \times \int_0^z \exp\left\{i\int_0^{z_2} [-q(z_1) + \Theta(z_0 - z)Q(z_1)]\,\mathrm{d}z_1\right\}\mathrm{d}z_2, \quad (9)$$

where the step-function $\Theta(z_0 - z)$ equals 1 and -1 if $z_0 - z > 0$ and $z_0 - z < 0$, respectively. Integrating by parts, one can replace the phase integral $\int_0^z Q(z_1)\,\mathrm{d}z_1$ by the expression $Q(z)z - \int_0^z Q'(z_1)z_1\,\mathrm{d}z_1$. It is clear that the former term is significant near z_0. As to the latter term, it can be reduced to the expression $-(\pi/\xi_g)^2\int_0^z p(z_1)p'(z_1)z_1\,\mathrm{d}z_1/Q(z_1)$, in which the small terms are neglected. This integral is appreciable only far from z_0, where we are able to suggest $Q(z) \approx (\pi/\xi_g)p(z)$. Then, it can be modified to the form $(-\pi/\xi_g)[zp(z) - \int_0^z p(z_1)\,\mathrm{d}z_1]$. Taking into consideration that $p(z) = |\eta(z)|$ far from z_0, we reduce this expression to the value $\varepsilon\pi^2 z^2\Theta(z_0 - z)/(2\xi_g^2)$. Hence, it is possible to obtain the following approximation for any z:

$$\int_0^z Q(z_1)\,\mathrm{d}z_1 \approx Q(z)z + (\mathbf{g}\cdot\mathbf{u}/2)\Theta(z_0 - z). \quad (10)$$

Substituting (10) into (9) and omitting the exponential factor which does not affect the diffracted intensity, one can get

$$D_g(\varsigma) = \frac{i}{\varepsilon}\int_0^{\varsigma} \exp\left\{i\left[-\frac{\omega}{\varepsilon} + \Theta(\varsigma_0 - \varsigma)Q(\varsigma)\right]\varsigma\right\} \mathrm{d}\varsigma. \qquad (11)$$

Here $\varsigma = \varepsilon\pi z/\xi_g$ is a dimensionless variable. It is interesting to point out that, when $\varsigma \gg \varsigma_0$, expression (11) tends to the special function $\Phi(i\varsigma^2)$, which coincides with the asymptotic of the rigorous solution for strong bending (Chukhovskii & Petrashen', 1977). This function corresponds as well to the kinematical diffraction limit, related with the single scattering of X-rays. Nevertheless, multiple scattering may be pronounced near z_0, even in the case of kinematical diffraction. It takes place in the specific mechanism of multibeam interchange in a strongly bent crystal, which is different from X-ray interference in a slightly deformed crystal. Indeed, considering a weak distortion, multiple interference is reduced to the into-a-branch contribution, associated with the amplitude modulation of the transmitted and diffracted waves. This effect produces *Pendellösung* fringes whose distances decrease with increasing curvature (Kato, 1964). On the other hand, for high bending, it follows from (7) and (11) that interbranch scattering produces a phase modulation of the wavefields, instead of an amplitude modulation. The effective period of the phase modulation occurring near z_0 can evidently be estimated by the interbranch extinction length $\Lambda_g = 2\xi_g/\varepsilon$. Since $\Lambda_g \ll \xi_g$, the X-ray scattering can be formally treated as a kinematical process. At the same time, by integrating in (11), the multiple interbranch scattering specified by the parameter $\varepsilon/p^2(\varsigma)$ will also be taken into account up to the highest-order approximations inclusively. Thus, within the given formalism we can calculate the influence of multiple scattering on the phases of the wavefields and determine the extinction features.

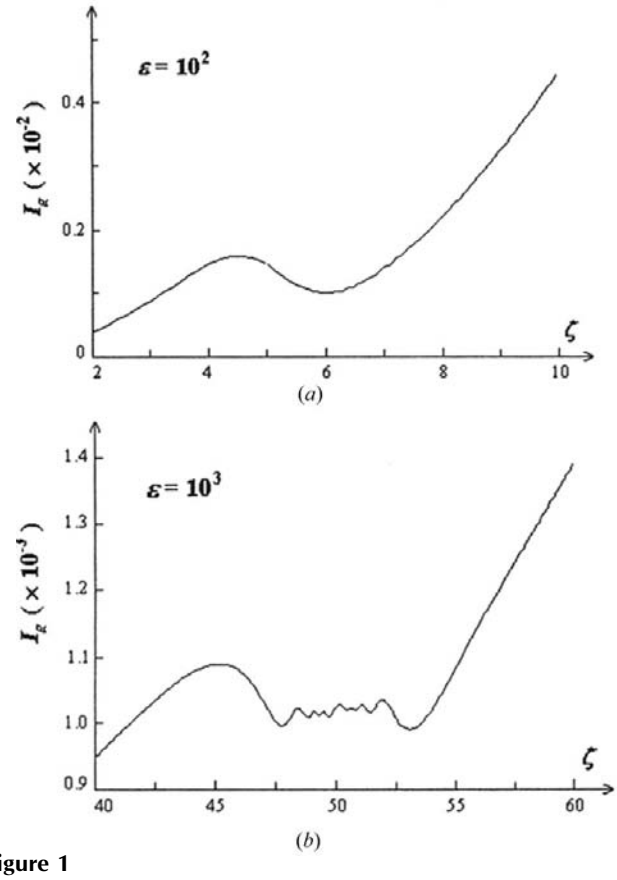

Figure 1
Variations of the diffracted intensities *versus* ς, near the points (*a*) $\varsigma_0 = 5$ and (*b*) $\varsigma_0 = 50$, which correspond to the depth $0.05\xi_g/\pi$.

3. Numerical results

The phase modulation caused by the interbranch processes may modify considerably the intensity of the diffracted wave I_g. Supposing high bending, we find the diffracted intensity $I_g(\varsigma) = |D_g(\varsigma)|^2$ by using expression (11) to demonstrate this effect. In this connection, the curves related to $\varepsilon = 10^2$ and $\varepsilon = 10^3$ are given in Figs. 1(*a*) and 1(*b*), respectively.

Both figures demonstrate clearly the oscillations of the diffracted intensity as a function of the crystal thickness. They are due to the interbranch phase changes and occur in the vicinity of the point where Bragg's condition is locally satisfied. Far from this point, oscillations disappear and the intensity tends towards the kinematical limit. Obviously, the spatial range of the interbranch oscillations, whose number grows with increasing ε, can be obtained from the estimations

$$p^2(\varsigma) \approx \frac{\varepsilon^2}{2p^4(\varsigma)}. \qquad (12)$$

From (12), it is easy to obtain the range of the oscillations $\Delta_{\rm int}(\varsigma) = 2|\varsigma - \varsigma_0| \approx 2(\varepsilon/2)^{1/3}$. For example, for the deformations $\varepsilon = 10^2$ and $\varepsilon = 10^3$, its magnitude is about 7.4 and 15.9 in units of $\xi_g/(\varepsilon\pi)$ or 1.2 and 2.5 in Λ_g, respectively, which correlates with the results presented in Fig. 1.

When calculating the X-ray rocking curve, one may expect as well a decrease of the intensity due to integration of the interbranch phase oscillations over the crystal thickness t in (11). Moreover, the deformation will cause a shift of the kinematical peak, which is equal to the value $\omega_M = -2\pi t/\Lambda_g$. In the case of $|\omega_M| \leq \Delta\omega_{1/2}$, where $\Delta\omega_{1/2} \approx \xi_g/t$ is the half-width of the rocking curve, the kinematical intensity is slowly changed at ω_M. Therefore, the interbranch losses of the intensity will be appreciable near this point. Far from ω_M, they

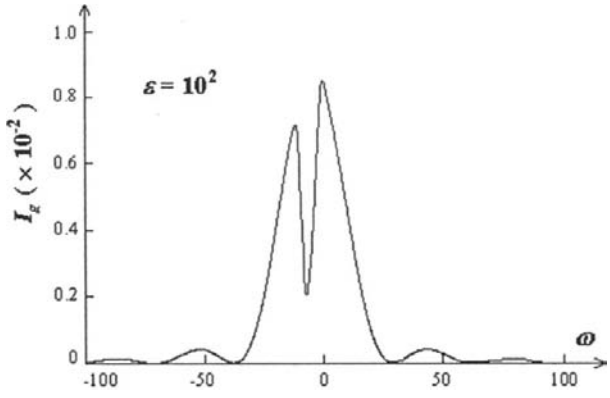

Figure 2
The rocking curve for $t = 1.5\Lambda_g$. The interbranch ratio is $\mu = 0.3$.

are minimal, since the interbranch transitions have to cease for the deviation $\omega \leq \omega_M$ and $\omega \geq 0$. Obviously, such a distribution of the intensity with ω implies its splitting at ω_M, which is verified in the calculated curve shown in Fig. 2.

It was also assumed that $\varepsilon = 10^2$ and $t = 1.5\Lambda_g$. This curve displays convincingly the interbranch splitting, the value of which can be estimated as $|\omega_M|$. In the angular units, the range of the splitting $\Delta Q_s = 2\pi|\omega_M|/(g\xi_g)$. It follows from this that $\Delta Q_s \approx 20''$ corresponds to Fig. 2 under the model parameters $\xi_g = 10^{-5}$ m and $g = 2\pi \times 10^{10}\,\mathrm{m}^{-1}$. It should also be noted that the interbranch splitting ΔQ_s increases with increasing deformation and can be of the order of angular minutes. To specify the interbranch features, it is convenient to take into consideration the ratio $\mu(\varepsilon, t) = |\omega_M|/\Delta\omega_{1/2}$. In the latter case, the interbranch ratio $\mu = 0.3 \leq 1$ indicates a splitting of the Bragg peak. As for the small additional peaks depicted in Fig. 2 and located beyond the range of the main peak, they are associated with the size effect, well known in kinematical diffraction (Krivoglaz, 1996).

In fact, the interbranch splitting is a size-related extinction effect, such that the angular splitting ΔQ_s depends on t. Along with this, not only the value of the interbranch effect but also the form of manifestation of this effect in the rocking curve can depend on the thickness, under the given deformation. This is illustrated by Figs. 3(*a*) and 3(*b*), which correspond to the deformation $\varepsilon = 10^3$. As one can see from the first figure, the interbranch splitting degenerates with increased values of t and μ. Furthermore, the interbranch anomaly is transformed into an asymmetrical broadening of the Bragg peak, while $t = 9\Lambda_g$ and $\mu = 1.0$. These modifications of the interbranch features are due to an increase of t, and consequently μ, such that the spatial range of the interbranch oscillations is sufficiently small in relation to the crystal thickness. Besides this, increasing thickness will be accompanied by an appropriate decrease of the half-width $\Delta\omega_{1/2}$ of the rocking curve, which changes sharply near ω_M. This means that the interbranch losses of the diffracted intensity will not be so prominent within the range of the diffraction maximum.

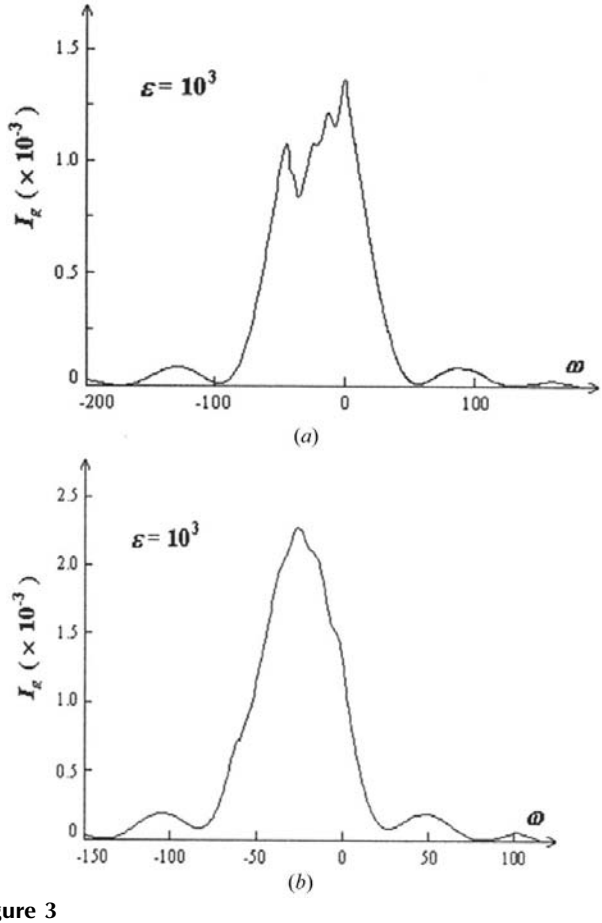

Figure 3
The rocking curves for (*a*) $t = 6.5\Lambda_g$ and (*b*) $t = 9\Lambda_g$, respectively. The appropriate interbranch ratios are $\mu = 0.5$ and $\mu = 1.0$.

It is natural to suggest that the described extinction effects can also be excited by the various long-range strain fields, which are capable of causing the X-ray interbranch crossover. Such displacements inherent in aged alloys, overgrown films and other strained-layer systems may induce intensive interbranch transitions. In this connection, the studies of Tanner & Hill (1986) and Barnett *et al.* (1989), which deal with the 'fine structure' effects in the rocking curve from strongly distorted heterostructures, should be pointed out. They reported that the superlattice-related diffraction peaks reveal a splitting and an asymmetrical broadening. It was also noted that the small size changes of the order 10^3 Å can influence markedly the rocking curve. Bearing in mind that the length Λ_g can be of the same order, it is possible to scale these changes in Λ_g and to interpret the features of the experimental curve as size-dependent interbranch peculiarities. One can hope as well that further investigation of the interbranch extinction anomalies could be useful to make progress towards the solution of the inverse problem and to give a deep insight into the theory of X-ray diffraction by non-ideal crystals.

4. Conclusions

Here we sum up the main results obtained in this work.

(i) It is derived from the Eikonal representation of the dynamical theory that the phase modulation of the transmitted and diffracted waves is attributed to interbranch processes in a strongly bent crystal. The effective modulation period is determined by the interbranch extinction length Λ_g.

(ii) The interbranch extinction effects, namely a splitting and an asymmetrical broadening, are deduced by analyzing the diffraction profile. They originate in the interbranch phase oscillations, excited near the point where the Bragg condition is locally satisfied.

(iii) It is established that the interbranch 'fine structure' of the rocking curve depends on the crystal thickness. With increasing thickness, the splitting of the Bragg peak degenerates and the interbranch peculiarity is transformed into asymmetrical broadening. Since the appropriate changes of the thickness are of the order of a few units of the interbranch

extinction length, which has a nano-sized value, the inter-branch features can be for X-ray nano-studies.

The author would like to thank Emeritus Professor Andre Authier for reviewing the manuscript and suggesting improvements.

References

Authier, A. (2005). *Dynamical Theory of X-ray Diffraction*. Oxford University Press.
Authier, A. & Balibar, F. (1970). *Acta Cryst.* A**26**, 647–654.
Balibar, F., Chukhovskii, F. N. & Malgrange, C. (1983). *Acta Cryst.* A**39**, 387–399.
Barnett, S. J., Brown, G. T., Houghton, D. C. & Baribeau, J.-M. (1989). *Appl. Phys. Lett.* **54**, 1781–1783.
Chukhovskii, F. N. & Petrashen', P. V. (1977). *Acta Cryst.* A**33**, 311–319.
Darwin, C. (1922). *Philos. Mag.* **43**, 800–829.
Hirsch, P., Howie, A., Nicolson, R., Pashley, D. & Whelan, M. (1977). *Electron Microscopy of Thin Crystals.* New York: Krieger.
Kato, N. (1964). *J. Phys. Soc. Jpn*, **19**, 971–985.
Krivoglaz, M. (1996). *Diffuse Scattering of X-rays and Neutrons by Fluctuations.* Berlin/Heidelberg/New York: Springer-Verlag.
Kuriyama, M. & Miyakawa, T. (1970). *Acta Cryst.* A**26**, 667–673.
Penning, P. (1966). PhD Thesis, Technical University of Delft, The Netherlands.
Shevchenko, M. (2005). *Acta Cryst.* A**61**, 512–515.
Shevchenko, M. & Pobydaylo, O. (2005). *J. Phys. D: Appl. Phys.* **38**, A232–A234.
Tanner, B. K. & Hill, M. (1986). *Adv. X-ray Anal.* **29**, 337–349.
Zachariasen, W. H. (1967). *Acta Cryst.* **23**, 558–564.